JOURNAL OF PROPULSION AND POWER
Vol. 15, No. 4, July–August 1999

Reduced Kinetics Mechanisms for Ram Accelerator Combustion

Eric L. Petersen* and Ronald K. Hanson†
Stanford University, Stanford, California 94305

Two skeletal kinetics mechanisms for reactive CH_4/O_2 and H_2/O_2 ram accelerator flowfields are presented. Both models were derived from a 190-reaction, 38-species kinetics mechanism (RAMEC or RAM accelerator MEChanism) that successfully reproduces the high-pressure (>50 atm), low-dilution (<70%), fuel-rich chemistry of ram accelerator mixtures. The reduction procedure for the CH_4/O_2 mechanism utilized a detailed-reduction technique with ignition delay time and heat release as the selection criteria. The methane-based mechanism (REDRAM or REDuced RAM accelerator mechanism) contains 34 reactions and 22 species and predicts ignition times to better than 5% and postcombustion temperatures to within 10 K of the full mechanism for a representative range of ram accelerator mixtures and conditions. This CH_4/O_2 mechanism is an improvement over existing reduced methane-oxidation mechanisms that are based on lower-pressure, higher-temperature chemistry. An 18-step, 9-species mechanism is presented for hydrogen-based ram accelerator combustion that is based on the H_2/O_2 submechanism of the RAMEC/Gas Research Institute GRI-Mech 1.2 methane-oxidation mechanism. The H_2/O_2 kinetics model includes HO_2 and H_2O_2 chemistry near the second and third explosion limits, necessary for ignition at ram accelerator pressures but lacking in certain finite rate chemistry models currently in use.

Introduction

THROUGHOUT the development of the ram accelerator concept, modeling of the complex flowfield has received particular attention. The high-pressure, reacting flowfield of the ram accelerator presents an ongoing challenge to numerical modelers, particularly in the interaction between chemistry and hydrodynamics. The ram accelerator, described in detail by Hertzberg et al.[1] and Bruckner et al.,[2] utilizes a projectile injected at supersonic speeds into a tube filled with a combustible mixture. Shock waves between the projectile body and the tube walls compress and heat the mixture; the ensuing combustion creates a pressure increase at the rear of the projectile, producing thrust that propels the projectile to very high speeds. The existence and location of the shock and/or detonation pattern depends on the velocity of the projectile relative to the Chapman–Jouguet speed of the mixture. Accurate numerical models of the reacting flow are needed in the design phase to ensure optimal heat release and thrust, avoiding, e.g., ignition in the forebody boundary layer.

Nonetheless, computational limitations force many numerical modelers to assume either equilibrium or one-step chemistry. For example, one-dimensional, control-volume-based gasdynamic models have been used with some success in predicting subdetonative ram accelerator performance,[1–3] but they are limited to equilibrium chemistry.[4] Early computational fluid dynamics (CFD) analyses assumed one-step, global reactions for both H_2/O_2-based[5] and CH_4/O_2-based[6] calculations. Oversimplified chemistry has certain drawbacks, however, including instantaneous conversion of reactants to products and overprediction of product temperatures.

Detailed chemical kinetics are required to model the true time-dependent nature of the combustion, particularly when predicting the distribution of heat release on the projectile body.[7] However, modern detailed kinetics mechanisms of hydrocarbon combustion can contain hundreds of reactions and dozens of species. The computational resources required to couple such a large reaction set to a full-scale numerical flow solver are excessive, rendering the use of such extensive mechanisms impractical at this time. As a compromise, many CFD simulations of ram accelerator flowfields incorporate multistep, finite rate chemistry in the form of a reduced mechanism, which captures essential aspects of the full mechanism.

A few numerical simulations of CH_4/O_2-based ram accelerator and related flowfields incorporating finite rate chemistry have been performed. In the work by Soetrisno et al.,[8,9] various methane-oxidation mechanisms were tested, with a 19-step, 13-species model giving the best results. Nusca and co-workers used a three-reaction model,[10,11] a four-step model,[12] and the 19-step mechanism of Soetrisno et al.[12] A 52-reaction kinetics model was employed by Yungster and Rabinowitz[13] to compute shock-induced combustion flowfields in stoichiometric CH_4/O_2 mixtures at Mach numbers near 6.

For H_2/O_2 mixtures, the pioneering work of Oran et al.[14] was among the first to marry multistep, finite rate chemistry with a numerical model of shock-induced H_2/O_2 combustion. More recently, Li et al.[15] employed a two-step reaction model to simulate oblique detonations on a ram accelerator, and a seven-species, eight-reaction reduced mechanism was used in numerical simulations of ram accelerator combustion by the authors of Refs. 16–19. Saurel[20] utilized an H_2/O_2 model that contained 19 reactions and 11 chemical species to simulate a ram accelerator with two-phase combustion. Yungster et al.[21] used the 19-step H_2/O_2 model of Jachimowski[22] to predict ram accelerator thrust.

Each of the previously mentioned numerical studies employed reduced mechanisms derived from the best chemical kinetics models available at that time. However, the original mechanisms were based mainly on low-pressure (1 atm), high-temperature (> 1400 K) data; whereas ram accelerators typically operate at pressures much greater than 50 atm (Ref. 23) and can achieve ignition within ram accelerator time scales at temperatures less than 1400 K. In addition, the ram accelerator fill gases are highly exothermic, often very rich mixtures of fuel and oxidizer with less than 70% dilution gas.[2,12,23] Prior to the shock-tube and kinetic-modeling studies in our laboratory, little was known about the validity of existing kinetics models when extrapolated to the harsh conditions of the ram accelerator.[24] The shock-tube ignition studies of Petersen et al.[25–27] provided the experimental data for validation and improvement of kinetics models at higher pressures and lower temperatures. Using these data as a guide, a detailed kinetics mechanism was developed that successfully models the ignition characteristics of typical ram accelerator mixtures at pressures approaching 300 atm (Ref. 28).

Presented as Paper 97-2892 at the AIAA/ASME/SAE/ASEE 33rd Joint Propulsion Conference, Seattle, WA, 6–9 July 1997; received 18 July 1998; revision received 29 October 1998; accepted for publication 4 November 1998.

*Graduate Research Assistant, Thermosciences Division, Department of Mechanical Engineering; currently Member of the Technical Staff, The Aerospace Corporation, El Segundo, CA 90245. Member AIAA.

†Professor, Thermosciences Division, Department of Mechanical Engineering. Fellow AIAA.

The purpose of the present study was to develop reduced mechanisms from the detailed model for use in numerical flowfield simulations. Both methane- and hydrogen-based reduced mechanisms were created. First, background information on the mechanism reduction procedure and the kinetics equations are provided. Details on both the CH_4/O_2 and H_2/O_2 mechanisms are presented in separate sections, and the predictive capabilities of each are shown in comparison with the original, full model and with some of the kinetics mechanisms used previously in CFD simulations of ram accelerator phenomena.

Background

Mechanism Reduction Procedure

Many techniques exist for the reduction of large chemical kinetics mechanisms, as summarized by Westbrook and Dryer,[29] Frenklach,[30] and Griffiths.[31] Three of the more commonly used methods are global modeling, response modeling, and detailed reduction.[30] In the global modeling approach, quasi-steady-state and partial equilibrium assumptions are used to reduce the full mechanism to one, two, or more steps that no longer represent elementary reactions, but rather represent some algebraic combination of the most significant steps. Specific examples of global mechanisms for hydrocarbon combustion systems can be found in Hautman et al.,[32] Jones and Lindstedt,[33] and the compilation edited by Peters and Rogg.[34]

Response modeling is the procedure wherein the full mechanism is solved over a range of temperatures, pressures, mixture ratios, etc., to establish the response of a particular variable such as ignition delay time or heat release. A mathematical expression representing the response variable as a function of the parameter space then takes the place of the full model in the numerical flow solver, reducing greatly the computation time. This technique has been used, for example, by Oran et al.[35] and Oran and Boris[36] for induction times, and Clifford et al.[37] for both induction time and energy release.

The detailed reduction approach retains the elementary-reaction format used in the full mechanism, leading to what is often referred to as a skeletal or quasiglobal model.[29] The full mechanism is reduced by eliminating reactions and species that have no influence on selected parameters such as induction time and/or the concentration of a key molecule. Examples of this technique can be found in Frenklach et al.,[38] Wang and Frenklach,[39] and Yungster and Rabinowitz.[13]

For the present study, detailed reduction was employed. Ignition delay time and final heat release were utilized as the selection criteria. The heat release was represented by the final equilibrium temperature after an adiabatic, constant-volume explosion. Reactions and species with little influence on the ignition delay time and final product temperature were systematically removed from the main mechanism, and brute force sensitivity analyses and sensitivity calculations using SENKIN[40] guided the elimination process. The final mechanisms are presented in later sections.

Chemical Kinetics

Because ram accelerator combustion can occur at very high pressures, the finite rate chemistry models should include pressure effects where applicable. The necessary relations for the pressure-dependent rate coefficients are summarized in this section.

The rate coefficients without pressure dependency take the conventional form:

$$k(T) = AT^n \exp(-E/RT) \tag{1}$$

where k is the rate coefficient in cm^3, mol, and s; A is a constant; T is the temperature in degrees Kelvin; E is the activation energy in cal/mol; and R is the universal gas constant (1.987 cal/mol-K). All chemical reactions herein are assumed to be reversible; the reverse reaction rate is calculated from the forward rate [Eq. (1)] and the equilibrium constant.

Unimolecular recombination (and decomposition) reactions involving collisions with a third body, M

$$A + B + M = AB + M \tag{2}$$

have pressure-dependent rate coefficients. For example, in the recombination direction

$$\frac{d[AB]}{dt} = k_{rec}(T, M)[A][B] \tag{3}$$

where $[X_i]$ is the concentration of species X_i, or $y_i P/RT$ for mole fraction y_i. The apparent second-order rate coefficient, $k_{rec}(T, M)$, is described by the Lindemann formulation:

$$k_{rec}(T, M) = k_\infty \left(\frac{k_0[M]}{k_0[M] + k_\infty} \right) \tag{4}$$

where $[M]$ is the total concentration of the mixture (or the concentration of a specific third-body such as N_2), including possible third-body collision efficiencies α_i:

$$[M] = \sum_{i=1}^{I} \alpha_i [X_i] \tag{5}$$

At low pressures, i.e., $[M] \to 0$, the rate is in the low-pressure limit and approaches $k_0(T)[M]$. When the reaction is in its high-pressure limit, i.e., $[M] \to \infty$, Eq. (4) becomes independent of M, or $k_{rec} = k_\infty(T)$. The form of $k_0(T)$ and $k_\infty(T)$ is given by Eq. (1). At densities between the low- and high-pressure limits, the reaction is in the falloff regime. The following equations defining the pressure-dependent rate coefficients follow the same format presented in Kee et al.[41]

For improved accuracy in the falloff regime,[42] Eq. (4) is usually modified by a factor F, and can be rearranged into the formula

$$k = k_\infty [P_r/(1 + P_r)]F \tag{6}$$

where P_r is the reduced pressure defined as

$$P_r = \frac{k_0[M]}{k_\infty} \tag{7}$$

The factor F in Eq. (6) is prescribed by the method of Troe[43]:

$$\ell n F = \left\{ 1 + \left[\frac{\ell n P_r + c}{n - d(\ell n P_r + c)} \right]^2 \right\}^{-1} \ell n F_c \tag{8}$$

The constants in Eq. (8) are given as

$$c = -0.4 - 0.67 \ell n(F_c) \tag{9}$$

$$n = 0.75 - 1.27 \ell n(F_c) \tag{10}$$

$$d = 0.14 \tag{11}$$

The Troe centering parameter, F_c, is

$$F_c = (1 - a)\exp(-T/T^{***}) + a\exp(-T/T^{*}) + \exp(-T^{**}/T) \tag{12}$$

For each reaction in the falloff regime, the four constants a, T^{***}, T^{*}, and T^{**} must be specified. Other techniques to fit the falloff region are available, but the authors selected the Troe method to comply with existing procedure in the larger mechanism.[28]

For reactions written in the dissociation direction, i.e., $AB + M = A + B + M$, the preceding equations are identical, with the exception that $k_{rec}(T, M)$ in Eq. (4) is replaced by $k_{diss}(T, M)$, and the corresponding rate expression becomes

$$\frac{d[A]}{dt} = \frac{d[B]}{dt} = k_{diss}(T, M)[AB] \tag{13}$$

Solution of the stiff set of ordinary differential rate equations was accomplished using Chemkin-II.[41] An ideal gas was assumed

for all calculations as it was shown previously for ram accelerator conditions and mixtures that ignition delay times obtained with a real-gas version of Chemkin[44] differed little from those obtained with the ideal-gas version.[28] To simulate ignition as it would occur in a ram accelerator mixture behind a reflected shock wave, the constant-volume, constant-internal-energy option in Chemkin was utilized, as in Petersen et al.[28]

Methane/Oxygen System

Previous Methane/Oxygen Work

A number of reduced methane oxidation mechanisms exist for the modeling of premixed and non-premixed flames, ignition delay times, and burning velocities. For example, Westbrook and Dryer,[29,45] Paczko et al.,[46] and Mauss and Peters[47] developed 1-, 2-, and 4-step global models for premixed methane–air flames using flame speed as the major response variable. In the compilation edited by Smooke,[48] a number of four-step global reactions for methane–air flames are presented. Ignition delay time was used to develop a six-step global mechanism by Treviño and Mendez[49] and an eight-step global mechanism by Gardiner et al.[50]

Reduced kinetics mechanisms compiled specifically for shock-induced CH_4/O_2 combustion problems include the 19-reaction model of Soetrisno et al.[8] and the 52-reaction model of Yungster and Rabinowitz.[13] The latter mechanism was derived from the 300-step mechanism of Frenklach et al.[51]

A major problem with applying existing mechanisms to ram accelerator flowfields is that most are based on (or were derived from larger models that were themselves based on) high-temperature flame, shock-tube, and flow-reactor data near 1 atm. The high-pressure, fuel-rich conditions of the ram accelerator are quite different, and difficulties often arise when using a reduced mechanism outside the parameter space for which it was designed.[45] Because ignition and heat release are the driving response variables for ram accelerator chemistry,[7] a mechanism based only on low-pressure burning velocities may not be the best choice. The conditions required for methane-based ram accelerator calculations are summarized in the following section.

Ram Accelerator Conditions (Methane/Oxygen)

The range of pressures, temperatures, and mixtures of interest herein are those observed in full-scale experiments at the Army Research Laboratory (ARL).[11,23,52] Both rich and lean mixtures have been tested at ARL, including the standard mixture $3CH_4 + 2O_2 + 10N_2$ ($\chi = 3$), a very fuel-rich mixture $6CH_4 + 2O_2 + 4He$ ($\chi = 6$), and a fuel-lean combination $0.4CH_4 + 2O_2 + 8N_2$ ($\chi = 0.4$). Although fill pressures vary between 50 and 100 atm, ignition generally occurs at higher pressures after the gas is processed by the bow shock wave. For an average projectile Mach number of 4 and a nose-cone half-angle between 10 and 14 deg, the pressure and temperature downstream of the bow shock ranges from 80–250 atm and 350–1300 K, depending on the fill pressure and proximity to the adiabatic boundary condition on the projectile body. Ignition delay time and finite rate kinetics are most important in this forebody region, where premature combustion can lead to a catastrophic unstart.[7] After the flow is further processed by near-normal shock wave(s), the pressure and temperature can reach hundreds of atmospheres and thousands of degrees Kelvin. The overall reaction quickly reaches chemical equilibrium at these extreme pressures and temperatures, i.e., the kinetics are extremely fast, and heat-release predictions become important.

Shock-tube measurements were performed in previous studies to quantify the ignition time characteristics of the ARL mixtures over a wide range of pressures (35–260 atm) and temperatures (1040–1600 K).[25,26] Existing high-temperature, low-pressure kinetics models were unable to reproduce the ignition trends seen in the shock-tube data, and so a detailed kinetics model, RAMEC (RAM accelerator MEChanism), was developed.[28] This 190-reaction, 38-species model contains additional reactions important at lower temperatures, higher pressures, and fuel-rich conditions, representing an improvement over the core CH_4/O_2 mechanism from the Gas Research Institute, GRI-Mech 1.2 (Ref. 53). For the purposes of this study, RAMEC is assumed to completely represent ram accelerator oxidation chemistry, providing a starting point and basis of comparison for mechanism reduction.

Reduced Methane/Oxygen Mechanism

A skeletal mechanism (REDRAM or REDuced RAM accelerator mechanism), containing 34 reactions and 22 species was derived from the detailed kinetics model. Table 1 summarizes REDRAM's reactions, species, and rate coefficients, and Table 2 lists the Troe constants for the six pressure-dependent reactions. The collision efficiencies for the three-body reactions are as used in RAMEC[28]; the exception is reaction R13, which is a combination of five separate rates, normalized via α_i to the rate coefficient for $H + O_2 + N_2 = HO_2 + N_2$. In Table 1, the inert species is assumed to be N_2, although any inert species such as helium or argon can be implemented instead. The thermodynamic data for the 22 species were those used in GRI-Mech 1.2 (Ref. 53), except for methyl peroxy (CH_3O_2), which was taken from the compilation of Burcat.[54]

Reactions R1–R15 and R32–R34 in Table 1 represent the buildup of radicals, and therefore, are the reactions that most influence ignition delay time. In general, the key radicals at ram accelerator conditions are CH_3 and HO_2, and the major chain-branching radicals are H and OH. At higher pressures and lower temperatures, methyl peroxy and hydrogen peroxide (H_2O_2) become important in the production of H and OH via R7–R11. The production of CH_3O_2 comes from R16, and the methane decomposition/recombination reaction (R17) is included for initiation. Reactions R32–R34 were added to REDRAM to obtain better agreement at fuel-lean conditions. In summary, the important branching reactions at higher pressures and lower temperatures accelerate the ignition chemistry, producing lower ignition times than expected from simply extrapolating lower pressure, higher temperature kinetics to the present conditions. Further details on ram accelerator CH_4/O_2 ignition chemistry can be found in Petersen et al.[25,26,28]

The remaining reactions are required for the complete oxidation of methane per the sequence:

$$\begin{array}{l} CH_4 \rightarrow CH_3 \rightarrow CH_3O \rightarrow CH_2O \rightarrow HCO \rightarrow CO \rightarrow CO_2 \\ \qquad\quad \downarrow \qquad\qquad\qquad\quad \uparrow \\ \qquad\quad C_2H_5 \rightarrow C_2H_4 \rightarrow C_2H_3 \end{array}$$

Formaldehyde production comes from two paths: 1) the decomposition of CH_3O via −R18 (also important for H-radical production); and 2) vinyl (C_2H_3) oxidation via R23, important for fuel-rich mixtures:

$$CH_3O + M = H + CH_2O + M \qquad (-R18)$$

$$C_2H_3 + O_2 = HCO + CH_2O \qquad (R23)$$

Vinyl formation begins with methyl recombination to ethyl (R19), followed by reactions (−R20) and (R22):

$$CH_3 + CH_3 = H + C_2H_5 \qquad (R19)$$

$$C_2H_5 + M = H + C_2H_4 + M \qquad (-R20)$$

$$CH_3 + C_2H_4 = C_2H_3 + CH_4 \qquad (R22)$$

Ethylene decomposition (R21) competes with (R22), forming the soot precursor acetylene:

$$C_2H_4 + M = H_2 + C_2H_2 + M \qquad (R21)$$

Although reactions involving collisions between C_2H_6 and C_2H_4 with OH radicals are important pathways for C_2H_3 production, they contribute little to heat release or ignition delay time and were not included in the reduced mechanism.

Fuel-rich formyl production comes from (R24), and fuel-lean HCO production is via (R25):

$$CH_3 + CH_2O = HCO + CH_4 \qquad (R24)$$

$$OH + CH_2O = HCO + H_2O \qquad (R25)$$

Table 1 Reduced kinetics mechanism for ram accelerator CH_4/O_2 combustion (REDRAM)

Number	Reaction[a]	Rate coefficient[b] A	n	E	Comments[c]
1	$CH_3 + CH_3 + M = C_2H_6 + M$	2.12×10^{16}	−1.00	620	k_{inf}, (R158)[d]
		1.77×10^{50}	−9.67	6,220	k_0
2	$CH_3 + O_2 = O + CH_3O$	2.68×10^{13}	0.00	28,800	(R155)
3	$CH_3 + O_2 = OH + CH_2O$	3.60×10^{10}	0.00	8,940	(R156)
4	$HO_2 + CH_3 = OH + CH_3O$	2.00×10^{13}	0.00	0	(R119)
5	$HO_2 + CH_3 = O_2 + CH_4$	1.00×10^{12}	0.00	0	(R118)
6	$O_2 + CH_2O = HO_2 + HCO$	1.00×10^{14}	0.00	40,000	(R32)
7	$CH_3 + H_2O_2 = HO_2 + CH_4$	2.45×10^{4}	2.50	5,180	(R157)
8	$HO_2 + CH_2O = H_2O_2 + HCO$	1.00×10^{12}	0.00	8,000	(R121)
9	$OH + OH + M = H_2O_2 + M$	7.40×10^{13}	−0.40	0	k_{inf}, (R85)[d]
		2.30×10^{18}	−0.90	−1,700	k_0
10	$HO_2 + HO_2 = O_2 + H_2O_2$	1.30×10^{11}	0.00	−1,630	k_a, (R115)[e]
		4.20×10^{14}	0.00	12,000	k_b, (R116)[e]
11	$CH_3O_2 + CH_3 = CH_3O + CH_3O$	3.00×10^{13}	0.00	−1,200	(R210)
12	$CH_3O + O_2 = HO_2 + CH_2O$	4.28×10^{-13}	7.60	−3,530	(R170)
13	$H + O_2 + M = HO_2 + M$	2.60×10^{19}	−1.20	0	(R33−R37)[f]
14	$H + O_2 = O + OH$	8.30×10^{13}	0.00	14,413	(R38)
15	$H + CH_4 = CH_3 + H_2$	6.60×10^{8}	1.60	10,840	(R53)
16	$CH_3 + O_2 = CH_3O_2$	1.70×10^{60}	−15.10	18,785	(R186)
17	$H + CH_3 + M = CH_4 + M$	1.27×10^{16}	−0.60	383	k_{inf}, (R52)[d]
		2.48×10^{33}	−4.76	2,440	k_0
18	$H + CH_2O + M = CH_3O + M$	5.40×10^{11}	0.50	2,600	k_{inf}, (R57)[d]
		2.20×10^{30}	−4.80	5,560	k_0
19	$CH_3 + CH_3 = H + C_2H_5$	4.99×10^{12}	0.10	10,600	(R159)
20	$H + C_2H_4 + M = C_2H_5 + M$	1.08×10^{12}	0.50	1,820	k_{inf}, (R74)[d]
		1.20×10^{42}	−7.62	6,970	k_0
21	$C_2H_4 + M = H_2 + C_2H_2 + M$	8.00×10^{12}	0.40	88,770	k_{inf}, (R174)[d]
		7.00×10^{50}	−9.31	99,860	k_0
22	$CH_3 + C_2H_4 = C_2H_3 + CH_4$	2.27×10^{5}	2.00	9,200	(R164)
23	$C_2H_3 + O_2 = HCO + CH_2O$	3.98×10^{12}	0.00	−240	(R173)
24	$CH_3 + CH_2O = HCO + CH_4$	3.32×10^{3}	2.80	5,860	(R161)
25	$OH + CH_2O = HCO + H_2O$	3.43×10^{9}	1.20	−447	(R101)
26	$HCO + O_2 = HO_2 + CO$	7.60×10^{12}	0.00	400	(R168)
27	$HCO + H_2O = H + CO + H_2O$	2.24×10^{18}	−1.00	17,000	(R167)
28	$HO_2 + CO = OH + CO_2$	1.50×10^{14}	0.00	23,600	(R120)
29	$OH + CO = H + CO_2$	4.76×10^{7}	1.20	70	(R99)
30	$OH + CH_4 = CH_3 + H_2O$	1.00×10^{8}	1.60	3,120	(R98)
31	$OH + OH = O + H_2O$	3.57×10^{4}	2.40	−2,110	(R86)
32	$O + CH_3 = H + CH_2O$	8.43×10^{13}	0.00	0	(R10)
33	$O + H_2 = H + OH$	5.00×10^{4}	2.70	6,290	(R3)
34	$H + H_2O_2 = HO_2 + H_2$	1.21×10^{7}	2.00	5,200	(R47)

Note: species = H_2, H, O, O_2, OH, H_2O, HO_2, H_2O_2, CH_3, CH_4, CO, CO_2, HCO, CH_2O, CH_3O, C_2H_2, C_2H_3, C_2H_4, C_2H_5, C_2H_6, N_2, and CH_3O_2.

[a]All reactions are reversible.

[b]$k(T) = AT^n \exp(-E/RT)$; units are in cal, mol, cm^3, and s.

[c]Corresponding RAMEC[28] reaction numbers are in parentheses.

[d]Collision efficiencies for M: $N_2 = 1.0$, $H_2 = 2.0$, $H_2O = 6.0$, $CH_4 = 2.0$, $CO = 1.5$, $CO_2 = 2.0$, $C_2H_6 = 3$, and $Ar = 0.7$, all others = 1.0.

[e]Rate coefficient is non-Arrhenius; $k_{10} = k_a + k_b$.

[f]Collision efficiencies for M: $N_2 = 1.0$, $O_2 = 0.3$, $H_2O = 7.0$, $CO = 0.75$, $CO_2 = 1.5$, $C_2H_6 = 1.5$, and $Ar = 0.5$, all others = 1.0.

Table 2 Troe parameters for pressure-dependent reactions

Reaction	a	T^{***}	T^{*}	T^{**}
1	0.5325	151	1038	4970
9[a]	0.7346	94	1756	5182
17	0.7830	74	2941	6964
18	0.7580	94	1555	4200
20	0.9753	210	984	4374
21	0.7345	180	1035	5417

[a]Same for reaction (r11) in Table 3.

Similarly, CO formation is via (R26) and (R27), with (R26) being more important for fuel-lean mixtures, and the conversion of CO to CO_2 follows primarily (R28) at rich conditions and (R29) at lean conditions:

$$HCO + O_2 = HO_2 + CO \quad \text{(R26)}$$

$$HCO + H_2O = H + CO + H_2O \quad \text{(R27)}$$

$$HO_2 + CO = OH + CO_2 \quad \text{(R28)}$$

$$OH + CO = H + CO_2 \quad \text{(R29)}$$

Reactions (R30) and (R31) are included in the reduced mechanism for the production of H_2O:

$$OH + CH_4 = CH_3 + H_2O \quad \text{(R30)}$$

$$OH + OH = O + H_2O \quad \text{(R31)}$$

Four reaction rate coefficients in REDRAM have a significant effect on the final equilibrium temperature. The rates of (R19) and (R20) (k_{19} and k_{20}, respectively) have the most individual impact, particularly at fuel-rich conditions, whereas k_{15} and k_{21} influence the product temperature to a lesser extent:

$$H + CH_4 = CH_3 + H_2 \quad \text{(R15)}$$

Results (Methane/Oxygen)

Ignition delay time calculations using REDRAM are presented in Figs. 1–3 along with predictions using the full mechanism (RAMEC), the 19-step reduced mechanism of Soetrisno et al.,[8] and the 52-step mechanism of Yungster and Rabinowitz.[13] The ignition delay times were determined from methane concentration profiles as the intersection of the steepest CH_4 decay with the original

concentration. This definition of τ_{ign} is convenient and agrees well with similar definitions based on pressure increase and radical formation.[55] Although the calculations in Figs. 1–3 are for a pressure of 150 atm, the quality of the results is representative of a ram accelerator ignition from 50 to 300 atm.

Results for the standard, fuel-rich ($\chi = 3$) ARL mixture are given in Fig. 1. Agreement between the reduced mechanism and the detailed mechanism is within 5% for temperatures between 1000 and 1500 K. The ignition times predicted by the Soetrisno et al. model[8] are too low by a factor of 3 at 1500 K, and too high by a factor of 10 at 1000 K. The Yungster and Rabinowitz mechanism[13] agrees well at the highest temperature (1500 K) but fails to encompass the lower-temperature, higher-pressure kinetics, overpredicting τ_{ign} by two orders of magnitude at 1000 K. However, the inaccuracies of the latter reduced mechanism are not surprising as it was based on lower pressure, higher-temperature CH_4-oxidation chemistry at near-stoichiometric conditions.

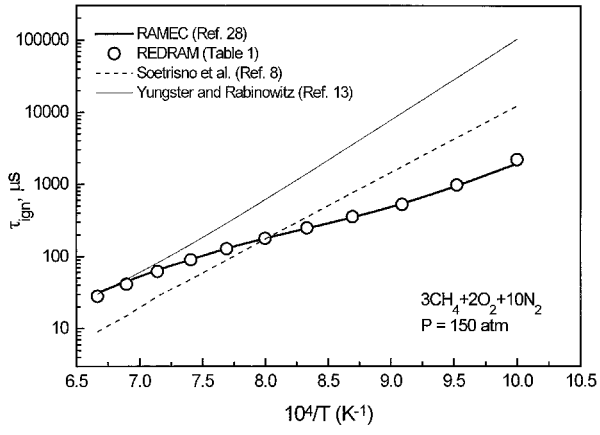

Fig. 1 Comparison between the CH_4/O_2 reduced mechanism (REDRAM) and the full mechanism (RAMEC) for the standard ARL mixture, $3CH_4 + 2O_2 + 10N_2$.

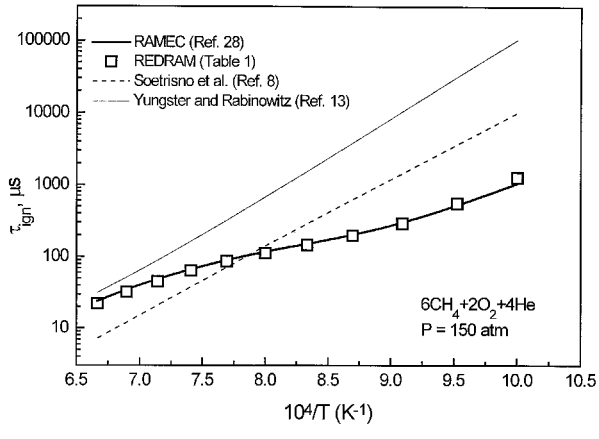

Fig. 2 Comparison between the CH_4/O_2 reduced mechanism (REDRAM) and the full mechanism (RAMEC) for the $6CH_4 + 2O_2 + 4He$ mixture.

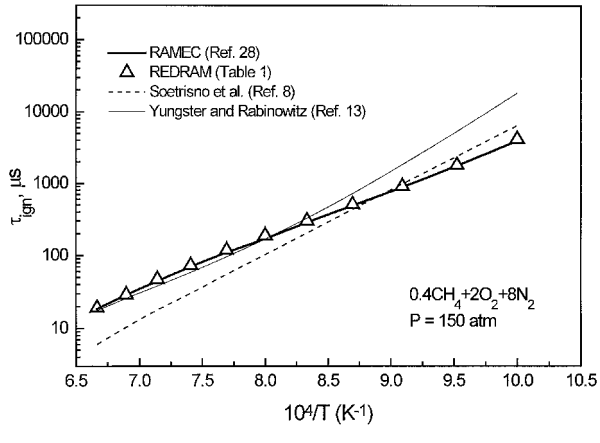

Fig. 3 Comparison between the CH_4/O_2 reduced mechanism (REDRAM) and the full mechanism (RAMEC) for the lean ARL mixture, $0.4CH_4 + 2O_2 + 8N_2$.

Similar agreement between REDRAM and the full mechanism is seen in Fig. 2 for a fuel-rich CH_4/O_2/He mixture with an equivalence ratio of 6. The ignition time predictions of the reduced mechanism are likewise good for the fuel-lean ($\chi = 0.4$) ARL mixture at 150 atm (Fig. 3), where the REDRAM τ_{ign} values are within 5% of RAMECs. Overall, the reduced mechanism provides ignition delay times that are essentially identical to those obtained using the 190-reaction model over the entire spectrum of ARL ram accelerator mixtures and conditions studied to date.

Excellent agreement is also found between the reduced and full mechanisms for the other design variable: heat release. For both rich and lean mixtures, REDRAM agrees within 10 K of the full mechanism at most pre-ignition temperatures. As expected, the error at slightly lean conditions is minor for each reduced mechanism.

Hydrogen/Oxygen System

Previous Hydrogen/Oxygen Studies

Because of its fundamental role in the combustion of most fuels there has been many studies concerning the H_2/O_2 reaction system. Many mechanisms have been compiled, e.g., Oran et al.,[14,35] Jachimowski,[22] Yetter et al.,[56] Balakrishnan and Williams,[57] etc., most of which contain fewer than 30 reactions. The multistage characteristics of hydrogen combustion[58] often benefit mechanism reduction by eliminating unimportant reactions. A typical reduced H_2/O_2 model is that proposed by Treviño,[59] who developed a five-step global mechanism.

Regarding ram accelerator numerical simulations, among the reduced mechanisms having the most influence on past calculations were those utilized by Evans and Schexnayder.[60] Two finite rate chemistry models were reported by Evans and Schexnayder: a 7-species, 8-step mechanism, and a 12-species, 25-step mechanism. The latter model includes reactions with nitrogen, and so only 8 species and 16 reactions involve exclusively H and O atoms. Many ram accelerator H_2/O_2 flowfields were simulated using the eight-reaction version,[16–19] while Saurel[20] opted for the larger model. The mechanism with eight reactions is representative of chain-branching H_2/O_2 kinetics at higher temperatures and lower pressures. Alternatively, the larger mechanism adds the key HO_2 radical, important for ignition at lower temperatures and higher pressures, but does not include reactions involving hydrogen peroxide. The implications of the two mechanisms at ram accelerator conditions are discussed in the following section.

Further ram accelerator numerical flow simulations were performed by Yungster et al.[21] using the 19-step mechanism of Jachimowski.[22] Jachimowski's H_2/O_2 mechanism contains a full set of reactions that includes both HO_2 and H_2O_2. A similar mechanism was compiled by Balakrishnan and Williams[57] and includes 21 reactions. Viguier et al.[61] utilized the Balakrishnan and Williams model in their numerical simulation of oblique detonation waves in stoichiometric H_2/O_2 mixtures.

Ram Accelerator Conditions (Hydrogen/Oxygen)

Most ram accelerator numerical studies have utilized one of three stoichiometric H_2/O_2 mixtures: $2H_2 + O_2 + 5He$ (Refs. 16–18 and 20), $2H_2 + O_2$ (Ref. 19), or $2H_2 + O_2 + 3.76N_2$, i.e., hydrogen/air.[15] For a 14-deg cone angle, fill pressures between 20 and 100 atm, and projectile Mach numbers between 7 and 9 (Refs. 19 and 20), the pressure downstream of the bow shock can reach 50–600 atm. The static temperature downstream of the bow shock is near 600 K, but the adiabatic wall temperature at the surface of the projectile can be higher than 3000 K. The actual temperature of the gas in the boundary-layer region is therefore between 600 and 3000 K. These high-pressure,

high-temperature conditions can lead to forebody combustion, the timing/location of which depends on the kinetics model employed. As discussed earlier for the CH_4/O_2-based mixtures, the pressure and temperature increase downstream of the near-normal shock(s) (close to the projectile midsection) in an H_2/O_2-based mixture lead to equilibrium conditions wherein the heat release portion of the chemistry is more important.

The ignition chemistry of H_2/O_2 mixtures depends greatly on the pressure and temperature.[58] For the current work, the H_2/O_2 subset of RAMEC,[28] i.e., that used in GRI-Mech 1.2 (Ref. 53), was assumed to fully represent the kinetics. This subset of the larger mechanism contains 28 elementary reactions and 10 species. Figure 4 presents ignition delay time predictions using RAMEC/GRI-Mech 1.2 for the $2H_2 + O_2 + 5He$ mixture over a range of representative pressures (1–600 atm) and temperatures (900–1300 K), assuming an adiabatic, constant-volume reaction. The results in Fig. 4, particularly for pressures greater than 50 atm, are based solely on kinetics calculations because few data exist at these high-pressure, high-temperature conditions.[62] The ignition-time characteristics change dramatically over such an extreme range of pressures. For example, τ_{ign} at 100 atm, 1100 K ($\approx$300 μs) is actually three times longer than τ_{ign} at 1 atm, 1100 K ($\approx$100 μs). This counterintuitive behavior is the result of distinct pressure- and temperature-dependent chemistry regimes. Viguier et al.[61] and Oran and Boris[36] describe similar H_2/O_2 ignition behavior at elevated pressures.

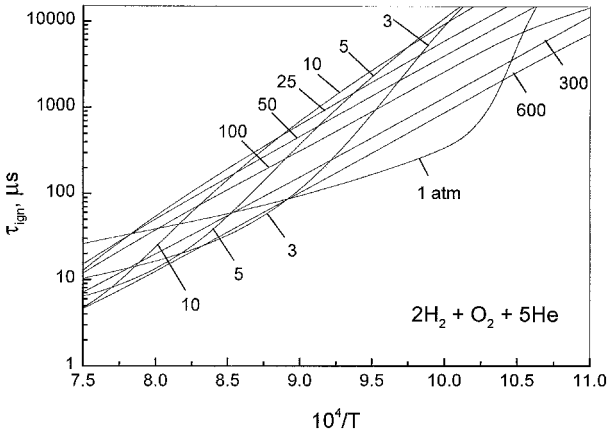

Fig. 4 Ignition delay time characteristics for the $2H_2 + O_2 + 5He$ mixture. The pressures represent preignition values. The curves shown are predictions based on the H_2/O_2 subset of the GRI mechanism, GRI-Mech 1.2. Note that experimental H_2/O_2 ignition data above ~ 10 atm are scarce or nonexistent.

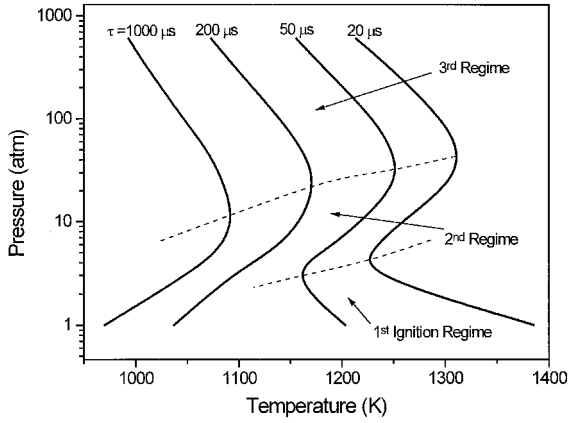

Fig. 5 Definition of ignition chemistry regimes for the $2H_2 + 2O_2 + 5He$ mixture. These curves were taken from lines of constant τ_{ign} in Fig. 4. The three regimes define regions in each ignition-time curve that exhibit similar kinetic behavior, i.e., temperature and pressure dependence. Similar curves exist for the other H_2/O_2 mixtures of interest. Refer to Fig. 4 for comments on the applicability and origin of the curves.

Figure 5 shows a P-T diagram where lines of constant ignition delay time are plotted. Each curve displays three separate ignition characteristics, or regimes, for the $2H_2 + O_2 + 5He$ mixture. At 1 atm and temperatures greater than 1100 K, ignition is dominated by the chain-branching reaction:

$$H + O_2 = O + OH \qquad (r6)$$

[To differentiate from reactions in the CH_4/O_2 system, which are designated by (R#), the H_2/O_2 reactions will be designated by a lower-case r, i.e. (r#).] The high-temperature, low-pressure portion of the ignition delay time curves (Fig. 5), where reaction (r6) is the most important step, will be referred to as the first ignition regime.

At intermediate pressures and lower temperatures, the competing reaction

$$H + O_2 + M = HO_2 + M \qquad (r2)$$

is the dominant step. The portion of the curves labeled 2nd regime in Fig. 5 characterizes the H_2/O_2 ignition behavior when (r2) is dominant. Reactions involving the HO_2 radical become more important, not only at lower temperatures, but also at higher pressures. Stoichiometric $H_2/O_2/Ar$ τ_{ign} data, presented by Petersen et al.,[27] clearly demonstrate the transition between the 1st and 2nd regimes at elevated pressures. This transition occurs at higher temperatures for increasing pressure where, by 3 atm, the $2H_2 + O_2 + 5He$ ignition chemistry is almost entirely within the 2nd (or 3rd) regime for the range of temperatures in Fig. 5. Reaction (r2) transitions from a termination step in the 1st and 2nd regimes to a propagating step at higher pressures.

For pressures greater than 50 atm in the $2H_2 + O_2 + 5He$ mixture, τ_{ign} follows yet a different trend, i.e., the slope in Fig. 4. This high-pressure characteristic signifies the 3rd ignition regime in the Fig. 5 curves. When ignition occurs in this 3rd regime, reactions involving hydrogen peroxide become important, with the dominant reaction being

$$HO_2 + H_2 = H + H_2O_2 \qquad (-r9)$$

According to Fig. 5, the 3rd ignition regime dominates the kinetics at ram accelerator pressures, and reactions involving H_2O_2 and HO_2 must be included in any reduced mechanism designed to predict ignition delay time. In contrast, the eight-step model of Evans and Schexnayder[60] (designed for high-temperature, 1-atm flowfields) does not include any reactions with HO_2 or H_2O_2. Although their 16-step mechanism includes HO_2, it does not include H_2O_2. Nonetheless, Evans and Schexnayder see significant differences in 1-atm flowfield simulations at low freestream temperatures when their mechanism with HO_2 is used instead of the eight-step mechanism without HO_2. By analogy, similar errors can occur at the higher pressures of the ram accelerator (where the HO_2 and H_2O_2 reactions are most important), if an inadequate chemistry model is used. A realistic reduced mechanism for H_2-fueled ram accelerator ignition, based on the rate coefficients used in RAMEC/GRI-Mech 1.2, was therefore developed.

Reduced Hydrogen/Oxygen Mechanism

The reduced H_2/O_2 mechanism contains 18 reactions and 9 species; the ninth specie is an inert gas such as nitrogen or helium. Table 3 presents the reactions, species, and reaction rate coefficients. For (r2), M signifies all molecules except O_2, H_2O, and N_2, which are represented by separate rate coefficients (r3–r5). The collision efficiencies for all other three-body reactions are cited in the table. The thermodynamic properties were taken from the Gas Research Institute mechanism.[53]

In the first ignition regime of each ignition-time curve (Fig. 5), the dominant promoters are the branching reactions (r1) and (r6):

$$O + H_2 = H + OH \qquad (r1)$$

$$H + O_2 = O + OH \qquad (r6)$$

Table 3 Suggested kinetics mechanism for ram accelerator H_2/O_2 combustion

Number	Reaction[a]	Rate coefficient[b] A	n	E	Comments[c]
1	$O + H_2 = H + OH$	5.00×10^4	2.70	6,290	(R3)
2	$H + O_2 + M = HO_2 + M$	2.80×10^{18}	−0.90	0	(R33)[d]
3	$H + O_2 + O_2 = HO_2 + O_2$	3.00×10^{20}	−1.70	0	(R34)
4	$H + O_2 + H_2O = HO_2 + H_2O$	9.38×10^{18}	−0.80	0	(R35)
5	$H + O_2 + N_2 = HO_2 + N_2$	2.60×10^{19}	−1.20	0	(R36)
6	$H + O_2 = O + OH$	8.30×10^{13}	0.00	14,413	(R38)
7	$H + HO_2 = O_2 + H_2$	2.80×10^{13}	0.00	1,068	(R45)
8	$H + HO_2 = OH + OH$	1.34×10^{14}	0.00	635	(R46)
9	$H + H_2O_2 = HO_2 + H_2$	1.21×10^7	2.00	5,200	(R47)
10	$OH + H_2 = H_2O + H$	2.16×10^8	1.50	3,430	(R84)
11	$OH + OH + M = H_2O_2 + M$	7.40×10^{13}	−0.40	0	k_{inf}, (R85)[e,f]
		2.30×10^{18}	−0.90	−1,700	k_0
12	$OH + HO_2 = O_2 + H_2O$	2.90×10^{13}	0.00	−500	(R87)
13	$OH + H_2O_2 = HO_2 + H_2O$	1.75×10^{12}	0.00	320	k_a, (R88)[g]
		5.80×10^{14}	0.00	9,560	k_b, (R89)[g]
14	$HO_2 + HO_2 = O_2 + H_2O_2$	1.30×10^{11}	0.00	−1,630	k_c, (R115)[h]
		4.20×10^{14}	0.00	12,000	k_d, (R116)[h]
15	$O + O + M = O_2 + M$	1.20×10^{17}	−1.00	0	(R1)[i]
16	$O + H + M = OH + M$	5.00×10^{17}	−1.00	0	(R2)[e]
17	$H + OH + M = H_2O + M$	2.20×10^{22}	−2.00	0	(R43)[j]
18	$H + H + M = H_2 + M$	1.00×10^{18}	−1.00	0	(R39)[k]

Note: species = H, O, OH, H_2, O_2, HO_2, H_2O_2, H_2O, and N_2 (or Ar, He, etc.).
[a] All reactions are reversible.
[b] $k(T) = AT^n \exp(-E/RT)$; units are in cal, mol, cm^3, and s.
[c] Corresponding RAMEC[28] reaction numbers are in parentheses.
[d] M does not include O_2, H_2O, or N_2; all collision efficiencies = 1.0.
[e] Collision efficiencies for M: $N_2 = 1.0$, $H_2 = 2.0$, $H_2O = 6.0$, and Ar = 0.70, all others = 1.0.
[f] See Table 2 for Troe parameters.
[g] Rate coefficient is non-Arrhenius; $k_{13} = k_a + k_b$.
[h] Rate coefficient is non-Arrhenius; $k_{14} = k_c + k_d$.
[i] Collision efficiencies for M: $N_2 = 1.0$, $H_2 = 2.4$, $H_2O = 15.4$, and Ar = 0.83, all others = 1.0.
[j] Collision efficiencies for M: $N_2 = 1.0$, $H_2 = 0.73$, $H_2O = 3.65$, and Ar = 0.38, all others = 1.0.
[k] Collision efficiencies for M: $N_2 = 1.0$, $H_2 = 1.7$, $H_2O = 7.0$, and Ar = 0.63, all others = 1.0.

and the major inhibitors are the reactions forming HO_2, (r2–r5):

$$H + O_2 + X = HO_2 + X, \qquad X = M, O_2, H_2O, N_2 \qquad \text{(r1–r5)}$$

Reactions (r8) and (r10) become significant ignition promoters in the 2nd and 3rd ignition regimes:

$$H + HO_2 = OH + OH \qquad \text{(r8)}$$

$$OH + H_2 = H + H_2O \qquad \text{(r10)}$$

In the 3rd ignition regime, the dominant promoter is the H_2O_2 formation reaction, (−r9), followed by importance by the subsequent decomposition of H_2O_2 (−r11) and the HO_2 formation reaction (−r7):

$$HO_2 + H_2 = H + H_2O_2 \qquad (-r9)$$

$$H_2O_2 + M = OH + OH + M \qquad (-r11)$$

$$O_2 + H_2 = H + HO_2 \qquad (-r7)$$

By far, the dominant inhibitor in the 3rd regime is the recombination of HO_2 (r14), which competes with the more-efficient H_2O_2 formation path (−r9):

$$HO_2 + HO_2 = O_2 + H_2O_2 \qquad \text{(r14)}$$

For dilute mixtures, such as in shock-tube studies, reactions (r12) and (r13) surface as ignition promoters at high pressures and low temperatures:

$$OH + HO_2 = O_2 + H_2O \qquad \text{(r12)}$$

$$OH + H_2O_2 = HO_2 + H_2O \qquad \text{(r13)}$$

At all conditions, water is formed almost solely via the reaction (r10) pathway. While only stoichiometric H_2/O_2 mixtures are shown herein, additional calculations have demonstrated that the Table 3 mechanism is similarly applicable to both lean and rich mixtures.

Results (Hydrogen/Oxygen)

Ignition delay time calculations using the reduced H_2/O_2 mechanism (Table 3) are presented in Fig. 6 for the $2H_2 + O_2$ mixture at four different pressures: 1, 10, 50, and 600 atm. Results obtained for the stoichiometric H_2/air and $2H_2 + O_2 + 5He$ mixtures are not shown herein, but are qualitatively similar to those provided in Fig. 6 for $2H_2 + O_2$. For the range of temperatures shown (850–1300 K), the reduced mechanism predicts ignition times identical to those of the full mechanism. At 50 and 600 atm, the reaction is well within the 3rd ignition regime (see Fig. 5). In general, τ_{ign} is less than 10 μs for temperatures greater than 1350 K.

At each pressure, the mechanisms of Jachimowski[22] and Balakrishnan and Williams[57] produce ignition trends that are similar to those from the RAMEC/GRI-Mech 1.2 mechanism. Nonetheless, while the high-temperature ignition times at 1 atm (first regime) are virtually identical, the mechanisms of Refs. 22 and 57 overpredict τ_{ign} in the second regime relative to RAMEC. The Jachimowski H_2/O_2 model agrees with RAMEC/GRI-Mech 1.2 within a factor of 2 in the 3rd ignition regime (Figs. 6b–6d), but the Balakrishnan and Williams model underpredicts τ_{ign} in the 3rd regime by a factor of 5 or more. Additional H_2/O_2 experimental ignition data at elevated pressures, particularly in the third ignition regime, are required to resolve any of the absolute differences seen in Fig. 6.

Significant discrepancies, however, are evident between the reduced mechanisms of Evans and Schexnayder[60] (which have incomplete chemistry in the second and third ignition regimes), and RAMEC/GRI-Mech 1.2. As expected, their eight-step mechanism is within a factor of 2 for the highest temperatures at 1 atm, i.e., in the 1st ignition regime. However, the eight-step model can lead to serious errors for temperatures less than ~1150 K, where semi-infinite ignition times are predicted. The results for the eight-step model are not even shown for the 50- and 600-atm plots because it predicts instantaneous ignition for $T > 1150$ K and no ignition for $T < 1150$ K. For the 16-step mechanism of Evans and Schexnayder, τ_{ign} is overpredicted by orders of magnitude at the lower

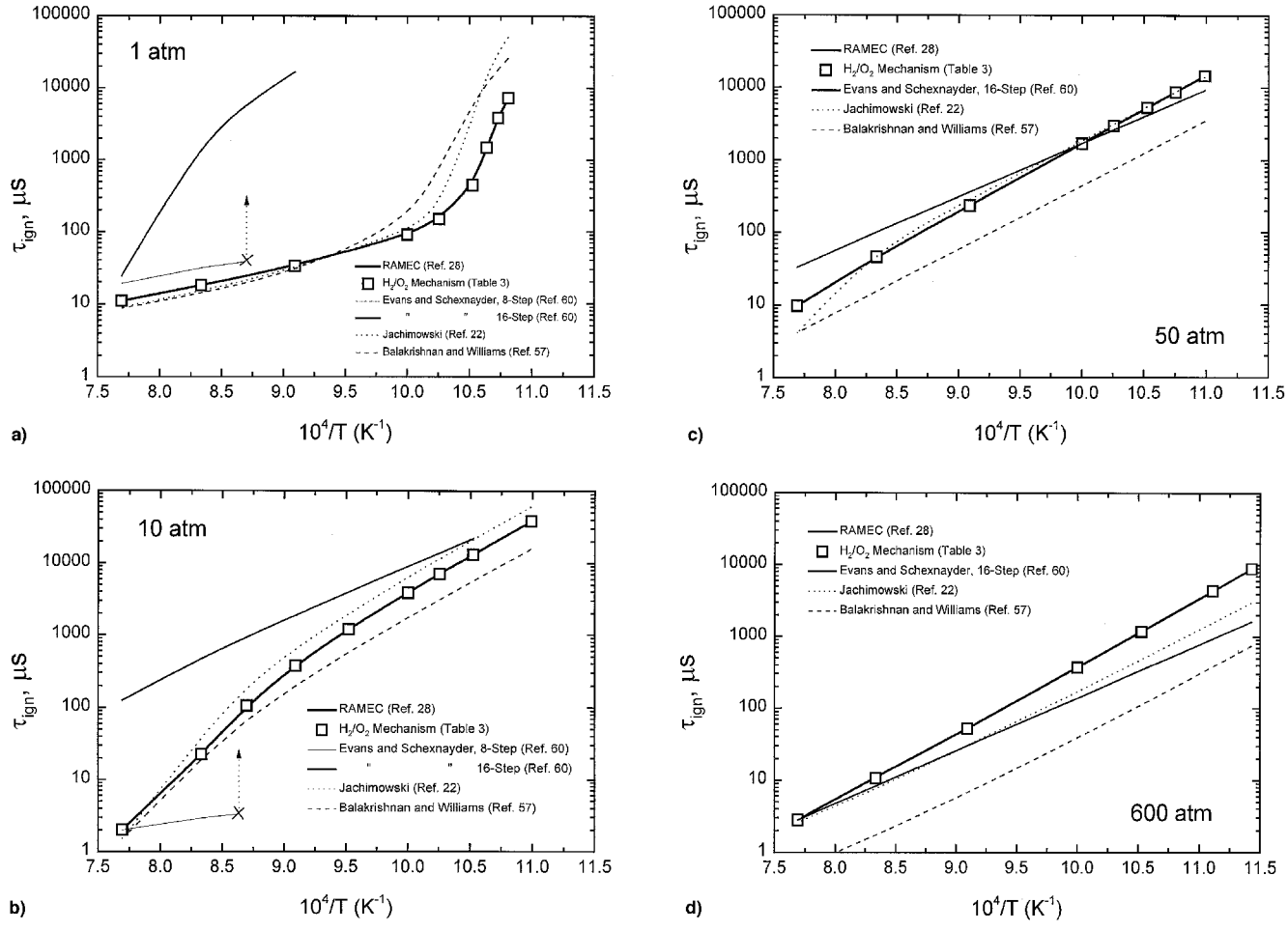

Fig. 6 Comparison between reduced H_2/O_2 mechanisms and the full mechanism (RAMEC/GRI-Mech 1.2) for the $2H_2 + O_2$ mixture. The eight-step Evans and Schexnayder[60] model predicts semi-infinite τ_{ign} for temperatures less than ~ 1150 K: a) 1 atm, b) 10 atm, c) 50 atm (few experimental H_2/O_2 ignition data are available in this pressure range), and d) 600 atm (no experimental H_2/O_2 ignition data exist in this pressure range).

pressures. Clearly, more reactions are not always better if the pathways are incorrect or the rate coefficients are outdated (Fig. 6a). The agreement between the Evans and Schexnayder 16-step model and RAMEC/GRI-Mech 1.2 at the higher pressures is better, although this may be fortuitous because hydrogen peroxide formation and decomposition, the most important paths in the third ignition regime, are not included in their model.

Excellent agreement between the current reduced mechanism (Table 3) and the full model is also seen for the prediction of post-combustion temperature. The temperature predicted using the reduced mechanism is identical to that of RAMEC. This result is expected for the stoichiometric ram accelerator mixtures because the only end product is water. Correct combustion temperatures are similarly calculated using an equilibrium assumption or the Evans and Schexnayder model.[60]

Discussion

The ultimate value of a reduced mechanism comes from its use in numerical flowfield simulations. An inadequate chemistry model can lead to a ram accelerator design that may unstart if the forebody ignition time is overpredicted; a seriously underpredicted ignition time can lead to an overdesigned ram accelerator projectile. Recent computational fluid dynamics simulations by Nusca[63] successfully employed REDRAM as the finite rate chemistry model. Nusca's results compare favorably with experiment and represent an improvement over earlier calculations that used incomplete chemistry. Nusca has also used the reduced H_2/O_2 model (Table 3) to simulate reactive flows over projectiles at conditions similar to those tested in the Stanford expansion tube facility.[63]

Additional work is required to develop reduced mechanisms with fewer species and reactions than those presented herein. For example, a global mechanism with less than 10 steps would further decrease the computational requirements. The tradeoff, of course, is the potential sacrifice in accuracy over some range of ram accelerator conditions. However, because most flowfield calculations involve one specific mixture (such as the standard ARL mixture, $3CH_4 + 2O_2 + 10N_2$) or configuration, separate reduced mechanisms can be tailored toward specific mixtures and conditions. Similarly, most of the reactions in Tables 1 and 3 are significant in only one direction, so that including simply the forward or reverse rate for such reactions would subsequently reduce computation times. Further mechanism reduction for the methane-based ram accelerator mixtures is in progress.[‡]

Of course, the accuracy of the reduced mechanisms is only as good as the rate coefficients that make up the full, detailed mechanism. While the 190-step RAMEC was based on the latest methane oxidation kinetics data (GRI-Mech 1.2, etc.), a number of rate coefficients important at higher pressures and lower temperatures are not well known.[28] In particular, the rate coefficients for the CH_3-oxidation reactions involving HO_2 have not been extensively studied. Likewise, HO_2 and H_2O_2 reactions in the H_2/O_2 submechanism near the 2nd and 3rd ignition regimes (Figs. 4 and 5) have rate coefficients with few, if any, measurements.[62,64] Errors in the rate coefficients can change the interpretation of the chemistry, eventually affecting dominant reactions that enter the reduced mechanism. When updated rate coefficient values and pathways are available, a new, modified mechanism should be developed and revalidated as appropriate.

[‡] Seshadri, K., Trees, D., and Anderson, W., personal communication, June 1997.

Conclusion

Using a detailed-reduction procedure with ignition delay time and heat release as the selection criteria, two reduced kinetics mechanisms for ram accelerator combustion were developed. Both reduced models were based on the 190-reaction, 38-species methane oxidation mechanism developed in an earlier study (RAMEC). Pressure-dependent rate coefficients were utilized where applicable. The first mechanism, REDRAM, contains 34 reactions and 22 species; it models ignition delay time for the methane-based ram accelerator mixtures. Ignition time predictions using REDRAM agree with the full mechanism within 5% for a range of mixture ratios ($\chi = 0.4$–6.0), pressures (50–300 atm), and temperatures (1000–1500 K), representing conditions downstream of the bow shock wave located on the projectile forebody. The reduced CH_4/O_2 mechanism also predicts the combustion product temperature within 10 K. When compared with previous finite rate chemistry models employed in numerical flowfield simulations of shock-induced combustion, REDRAM represents an improvement, particularly for rich mixtures at elevated pressures.

The second reduced kinetics mechanism was developed for hydrogen-based ram accelerator combustion. Calculations using the full mechanism indicate ram accelerator H_2/O_2 ignition occurs primarily in a regime where high-pressure pathways dominate. Large errors in the ignition delay time can occur if chemistry models do not incorporate reactions involving H_2O_2 and HO_2. The final H_2/O_2 reduced model has 18 reactions and 9 species. Comparisons with RAMEC/GRI-Mech 1.2 indicate that the reduced mechanism predictions of ignition time and heat release are identical to those of the full mechanism for typical ram accelerator mixtures ($2H_2 + O_2$, etc.) and postshock pressures (50–600 atm). Comparisons between REDRAM and other detailed H_2/O_2 kinetics models[22,57] show similar trends, but the actual value of ignition delay time at elevated pressures can differ by a factor of 5 or more, demonstrating the need for further high-pressure H_2/O_2 ignition experiments to anchor the chemistry.

Acknowledgments

This work was funded by the Army Research Office, with David Mann as the Technical Monitor, and by the Office of Naval Research, with Richard Miller as the Technical Monitor.

References

[1]Hertzberg, A., Bruckner, A. P., and Bogdanoff, D. W., "Ram Accelerator: A New Chemical Method for Accelerating Projectiles to Ultrahigh Velocities," *AIAA Journal*, Vol. 26, No. 2, 1988, pp. 195–203.

[2]Bruckner, A. P., Knowlen, C., Hertzberg, A., and Bogdanoff, D. W., "Operational Characteristics of the Thermally Choked Ram Accelerator," *Journal of Propulsion and Power*, Vol. 7, No. 5, 1991, pp. 828–836.

[3]Buckwalter, D. L., Knowlen, C., and Bruckner, A. P., "Ram Accelerator Performance Analysis Code Incorporating Real Gas Effects," AIAA Paper 96-2945, July 1996.

[4]Liberatore, F., "One-Dimensional, Equilibrium-Chemistry Ram Accelerator Performance Calculations," *Journal of Propulsion and Power*, Vol. 11, No. 6, 1995, pp. 1366–1368.

[5]Brackett, D. C., and Bogdanoff, D. W., "Computational Investigation of Oblique Detonation Ramjet-in-Tube Concepts," *Journal of Propulsion and Power*, Vol. 5, No. 3, 1989, pp. 276–281.

[6]Nusca, M., "Numerical Simulation of Reacting Flow in a Thermally Choked Ram Accelerator Projectile Launch System," AIAA Paper 91-2490, June 1991.

[7]Nusca, M. J., "Reacting Flow Simulation of Transient Multi-Stage Ram Accelerator Operation and Design Studies," AIAA Paper 95-2494, July 1995.

[8]Soetrisno, M., Imlay, S. T., and Roberts, D. W., "Numerical Simulations of the Transdetonative Ram Accelerator Combusting Flow Field on a Parallel Computer," AIAA Paper 92-3249, July 1992.

[9]Soetrisno, M., Imlay, S. T., and Roberts, D. W., "Numerical Simulations of the Superdetonative Ram Accelerator Combusting Flow Field," AIAA Paper 93-2185, June 1993.

[10]Nusca, M. J., "Numerical Simulation of Fluid Dynamics with Finite-Rate and Equilibrium Combustion Kinetics for the 120-mm Ram Accelerator," AIAA Paper 93-2182, June 1993.

[11]Nusca, M. J., and Kruczynski, D. L., "Reacting Flow Simulation for a Large-Scale Ram Accelerator," *Journal of Propulsion and Power*, Vol. 12, No. 1, 1996, pp. 61–69.

[12]Nusca, M. J., "Investigation of Ram Accelerator Flows for High Pressure Mixtures of Various Chemical Composition," AIAA Paper 96-2946, July 1996.

[13]Yungster, S., and Rabinowitz, M. J., "Computation of Shock-Induced Combustion Using a Detailed Methane-Air Mechanism," *Journal of Propulsion and Power*, Vol. 10, No. 5, 1994, pp. 609–617.

[14]Oran, E. S., Young, T. R., Boris, J. P., and Cohen, A., "Weak and Strong Ignition. I. Numerical Simulations of Shock Tube Experiments," *Combustion and Flame*, Vol. 48, 1982, pp. 135–148.

[15]Li, C., Kailasanath, K., Oran, E. S., Landsberg, A. M., and Boris, J. P., "Dynamics of Oblique Detonations in Ram Accelerators," *Shock Waves*, Vol. 5, No. 1/2, 1995, pp. 97–101.

[16]Yungster, S., Eberhardt, S., and Bruckner, A. P., "Numerical Simulation of Hypervelocity Projectiles in Detonable Gases," *AIAA Journal*, Vol. 29, No. 2, 1991, pp. 187–199.

[17]Yungster, S., "Numerical Study of Shock-Wave/Boundary-Layer Interactions in Premixed Combustible Gases," *AIAA Journal*, Vol. 30, No. 10, 1992, pp. 2379–2387.

[18]Yungster, S., and Bruckner, A. P., "Computational Studies of a Superdetonative Ram Accelerator Mode," *Journal of Propulsion and Power*, Vol. 8, No. 2, 1992, pp. 457–463.

[19]Dyne, B. R., and Heinrich, J. C., "Finite Element Analysis of the Scram-accelerator with Hydrogen-Oxygen Combustion," *Journal of Propulsion and Power*, Vol. 12, No. 2, 1996, pp. 336–340.

[20]Saurel, R., "Numerical Analysis of a Ram Accelerator Employing Two-Phase Combustion," *Journal of Propulsion and Power*, Vol. 12, No. 4, 1996, pp. 708–717.

[21]Yungster, S., Radhakrishnan, K., and Rabinowitz, M. J., "Reacting Flow Establishment in Ram Accelerators: A Numerical Study," *Journal of Propulsion and Power*, Vol. 14, No. 1, 1998, pp. 10–17.

[22]Jachimowski, C. J., "An Analytical Study of the Hydrogen-Air Reaction Mechanism with Application to Scramjet Combustion," NASA TP 2791, Feb. 1988.

[23]Kruczynski, D. L., "New Experiments in a 120-mm Ram Accelerator at High Pressures," AIAA Paper 93-2589, June 1993.

[24]Anderson, W. R., and Kotlar, A. J., "Detailed Modeling of CH_4/O_2 Combustion for Hybrid In-Bore Ram Propulsion (HIRAM) Application," *28th JANNAF Combustion Subcommittee Meeting*, Vol. 2, Chemical Propulsion Information Agency, Publ. 573, 1991, pp. 417–426.

[25]Petersen, E. L., Davidson, D. F., and Hanson, R. K., "Ignition Delay Times of Ram Accelerator CH_4/O_2/Diluent Mixtures," *Journal of Propulsion and Power*, Vol. 15, No. 1, 1999, pp. 82–91.

[26]Petersen, E. L., Davidson, D. F., and Hanson, R. K., "Ram Accelerator Mixture Chemistry: Kinetics Modeling and Ignition Measurements," *1996 JANNAF Combustion Subcommittee Meeting*, Vol. 1, Chemical Propulsion Information Agency, Publ. 653, 1997, pp. 395–407.

[27]Petersen, E. L., Davidson, D. F., Röhrig, M., and Hanson, R. K., "High-Pressure Shock-Tube Measurements of Ignition Times in Stoichiometric H_2/O_2/Ar Mixtures," *Shock Waves—Proceedings of the 20th International Symposium on Shock Waves*, edited by B. Sturtevant, J. Shephard, and H. G. Hornung, World Scientific, River Edge, NJ, 1996, pp. 941–946.

[28]Petersen, E. L., Davidson, D. F., and Hanson, R. K., "Kinetics Modeling of Shock-Induced Ignition in Low-Dilution CH_4/O_2 Mixtures at High Pressures and Intermediate Temperatures," *Combustion and Flame*, Vol. 117, No. 1–2, 1999, pp. 272–290.

[29]Westbrook, C. K., and Dryer, F. L., "Simplified Reaction Mechanisms for the Oxidation of Hydrocarbon Fuels in Flames," *Combustion Science and Technology*, Vol. 27, No. 1–2, 1981, pp. 31–43.

[30]Frenklach, M., "Reduction of Chemical Reaction Models," *Numerical Approaches to Combustion Modeling*, edited by E. S. Oran and J. P. Boris, Vol. 135, Progress in Astronautics and Aeronautics, AIAA, Washington, DC, 1991, pp. 129–154.

[31]Griffiths, J. F., "Reduced Kinetic Models and Their Application to Practical Combustion Systems," *Progress in Energy and Combustion Science*, Vol. 21, 1995, pp. 25–107.

[32]Hautman, D. J., Dryer, F. L., Schug, K. P., and Glassman, I., "A Multiple-Step Overall Kinetic Mechanism for the Oxidation of Hydrocarbons," *Combustion Science and Technology*, Vol. 25, No. 5, 6, 1981, pp. 219–235.

[33]Jones, W. P., and Lindstedt, R. P., "Global Reaction Schemes for Hydrocarbon Combustion," *Combustion and Flame*, Vol. 73, 1988, pp. 233–249.

[34]Peters, N., and Rogg, B. (ed.), *Reduced Kinetic Mechanisms for Applications in Combustion Systems*, Springer–Verlag, Berlin, 1993.

[35]Oran, E. S., Boris, J. P., Young, T., Flanigan, M., Burks, T., and Picone, M., "Numerical Simulations of Detonations in Hydrogen-Air and Methane-Air Mixtures," *18th Symposium (International) on Combustion*, The Combustion Inst., Pittsburgh, PA, 1981, pp. 1641–1649.

[36]Oran, E. S., and Boris, J. P., "Weak and Strong Ignition. II. Sensitivity of the Hydrogen-Oxygen System," *Combustion and Flame*, Vol. 48, 1982, pp. 149–161.

[37]Clifford, L. J., Milne, A. M., and Murray, B. A., "Numerical Modeling of Chemistry and Gas Dynamics During Shock-Induced Ethylene Combustion," *Combustion and Flame*, Vol. 104, No. 3, 1996, pp. 311–327.

[38]Frenklach, M., Kailasanath, K., and Oran, E. S., "Systematic Development of Reduced Reaction Mechanisms for Dynamic Modeling," *Dynamics of Reactive Systems Part II: Modeling and Heterogeneous Combustion*, edited by J. R. Bowen, J.-C. Leyer, and R. I. Soloukhin, Vol. 105, Progress in Astronautics and Aeronautics, AIAA, New York, 1986, pp. 365–376.

[39]Wang, H., and Frenklach, M., "Detailed Reduction of Reaction Mechanisms for Flame Modeling," *Combustion and Flame*, Vol. 87, No. 3, 4, 1991, pp. 365–370.

[40]Lutz, A. E., Kee, R. J., and Miller, J. A., "SENKIN: A Fortran Program for Predicting Homogeneous Gas Phase Chemical Kinetics with Sensitivity Analysis," Sandia National Labs., SAND87-8248, Livermore, CA, 1988.

[41]Kee, R. J., Rupley, F. M., and Miller, J. A., "Chemkin-II: A Fortran Chemical Kinetics Package for the Analysis of Gas-Phase Chemical Kinetics," Sandia National Labs., SAND89-8009, Livermore, CA, 1989.

[42]Larson, C. W., Patrick, R., and Golden, D. M., "Pressure and Temperature Dependence of Unimolecular Bond Fission Reactions: An Approach for Combustion Modelers," *Combustion and Flame*, Vol. 58, No. 3, 1984, pp. 229–237.

[43]Troe, J., "Predictive Possibilities of Unimolecular Rate Theory," *Journal of Physical Chemistry*, Vol. 83, No. 1, 1979, pp. 114–126.

[44]Schmitt, R. G., Butler, P. B., and French, N. B., "Chemkin Real Gas: A Fortran Package for Analysis of Thermodynamic Properties and Chemical Kinetics in Nonideal Systems," Univ. of Iowa, UIME PBB 93-006, Iowa City, IA, Dec. 1993.

[45]Westbrook, C. K., and Dryer, F. L., "Chemical Kinetic Modeling of Hydrocarbon Combustion," *Progress in Energy and Combustion Science*, Vol. 10, No. 1, 1984, pp. 1–57.

[46]Paczko, G., Lefdal, P. M., and Peters, N., "Reduced Reaction Schemes for Methane, Methanol, and Propane Flames," *21st Symposium (International) on Combustion*, The Combustion Inst., Pittsburgh, PA, 1986, pp. 739–748.

[47]Mauss, F., and Peters, N., "Reduced Kinetic Mechanisms for Premixed Methane-Air Flames," *Reduced Kinetic Mechanisms for Applications in Combustion Systems*, edited by N. Peters and B. Rogg, Springer–Verlag, Berlin, 1993, pp. 58–75.

[48]Smooke, M. D. (ed.)., *Reduced Kinetic Mechanisms and Asymptotic Approximations for Methane-Air Flames*, Springer–Verlag, Berlin, 1991.

[49]Treviño, C., and Mendez, F., "Reduced Kinetic Mechanism for Methane Ignition," *24th Symposium (International) on Combustion*, The Combustion Inst., Pittsburgh, PA, 1992, pp. 121–127.

[50]Gardiner, W. C., Jr., Lissianski, V. V., and Zamanski, V. M., "Reduced Chemical Reaction Mechanism of Shock-Initiated Ignition of Methane and Ethane Mixtures with Oxygen," *Shock Waves @ Marseille II*, edited by R. Brun and L. Z. Dumitrescu, Springer–Verlag, Berlin, 1995, pp. 155–160.

[51]Frenklach, M., Wang, H., and Rabinowitz, M. J., "Optimization and Analysis of Large Chemical Kinetic Mechanisms Using the Solution Mapping-Combustion of Methane," *Progress in Energy and Combustion Science*, Vol. 18, 1992, pp. 47–73.

[52]Kruczynski, D. L., and Liberatore, F., "Ram Accelerator Experiments with Unique Projectile Geometries," AIAA Paper 95-2490, July 1995.

[53]Frenklach, M., Wang, H., Goldenberg, M., Smith, G. P., Golden, D. M., Bowman, C. T., Hanson, R. K., Gardiner, W. C., and Lissianski, V., "GRI-Mech—An Optimized Detailed Chemical Reaction Mechanism for Methane Combustion," Gas Research Inst., Topical Rept. GRI-95/0058, Chicago, IL, Nov. 1995.

[54]Burcat, A., "Thermochemical Data for Combustion Calculations," *Combustion Chemistry*, edited by W. C. Gardiner Jr., Springer–Verlag, New York, 1984, pp. 455–473.

[55]Petersen, E. L., Röhrig, M., Davidson, D. F., Hanson, R. K., and Bowman, C. T., "High-Pressure Methane Oxidation Behind Reflected Shock Waves," *26th Symposium (International) on Combustion*, The Combustion Inst., Pittsburgh, PA, 1996, pp. 799–806.

[56]Yetter, R. A., Rabitz, H., and Hedges, R. M., "A Combined Stability-Sensitivity Analysis of Weak and Strong Reactions of Hydrogen/Oxygen Mixtures," *International Journal of Chemical Kinetics*, Vol. 23, No. 3, 1991, pp. 251–278.

[57]Balakrishnan, G., and Williams, F. A., "Turbulent Combustion Regimes for Hypersonic Propulsion Employing Hydrogen-Air Diffusion Flames," *Journal of Propulsion and Power*, Vol. 10, No. 3, 1993, pp. 434–437.

[58]Glassman, I., *Combustion*, Academic, Orlando, FL, 1987, pp. 56–63.

[59]Treviño, C., "Ignition Phenomena in H_2-O_2 Mixtures," *Dynamics of Deflagrations and Reactive Systems: Flames*, edited by A. L. Kuhl, J.-C. Leyer, A. A. Borisov, and W. A. Sirignano, Vol. 131, Progress in Astronautics and Aeronautics, AIAA, New York, 1990, pp. 19–43.

[60]Evans, J. S., and Schexnayder, C. J., Jr., "Influence of Chemical Kinetics and Unmixedness on Burning in Supersonic Hydrogen Flames," *AIAA Journal*, Vol. 18, No. 2, 1980, pp. 188–193.

[61]Viguier, C., Da Silva, L. F. F., Desbordes, D., and Deshaies, B., "Onset of Oblique Detonation Waves: Comparison Between Experimental and Numerical Results for Hydrogen-Air Mixtures," *26th Symposium (International) on Combustion*, The Combustion Inst., Pittsburgh, PA, 1996, pp. 3023–3031.

[62]Lee, D., and Hochgreb, S., "Hydrogen Autoignition at Pressures Above the Second Explosion Limit (0.6-4.0 Mpa)," *International Journal of Chemical Kinetics*, Vol. 30, No. 6, 1998, pp. 385–406.

[63]Nusca, M. J., "Computational Simulation of the Ram Accelerator Using a Coupled CFD/Interior Ballistic Approach," AIAA Paper 97-2653, July 1997.

[64]Kim, T. J., Yetter, A., and Dryer, F. L., "New Results on Moist CO Oxidation: High Pressure, High Temperature Experiments and Comprehensive Kinetic Modeling," *25th Symposium (International) on Combustion*, The Combustion Inst., Pittsburgh, PA, 1994, pp. 759–766.